

Generalized cold-atom simulators for vacuum decay

Alexander C. Jenkins^{1,*}, Ian G. Moss², Thomas P. Billam³,
Zoran Hadzibabic⁴, Hiranya V. Peiris^{5,6} and Andrew Pontzen¹

¹*Department of Physics and Astronomy, University College London, London WC1E 6BT, UK*

²*School of Mathematics, Statistics and Physics, Newcastle University, Newcastle upon Tyne, NE1 7RU, UK*

³*Joint Quantum Centre (JQC) Durham–Newcastle, School of Mathematics,
Statistics and Physics, Newcastle University, Newcastle upon Tyne, NE1 7RU, UK*

⁴*Cavendish Laboratory, University of Cambridge,
J. J. Thomson Avenue, Cambridge CB3 0HE, UK*

⁵*Institute of Astronomy and Kavli Institute for Cosmology, Madingley Road, Cambridge, CB3 0HA, UK*

⁶*The Oskar Klein Centre for Cosmoparticle Physics, Department of Physics,
Stockholm University, AlbaNova, Stockholm, SE-106 91, Sweden*

(Dated: 7 November 2023)

Cold-atom analogue experiments are a promising new tool for studying relativistic vacuum decay, allowing us to empirically probe early-Universe theories in the laboratory. However, existing analogue proposals place stringent requirements on the atomic scattering lengths that are challenging to realize experimentally. Here we generalize these proposals and show that *any* stable mixture between two states of a bosonic isotope can be used as a relativistic analogue. This greatly expands the range of suitable experimental setups, and will thus expedite efforts to study vacuum decay with cold atoms.

Introduction.—Quantum fields can escape from meta-stable ‘false vacuum’ states via the spontaneous nucleation of ‘true vacuum’ bubbles [1–5]. This process of *vacuum decay* plays a pivotal role in many aspects of cosmology, from the Universe’s inflationary beginnings [6–10] to the present-day (meta)stability of the Higgs field [11–13]. The standard analytical treatment of this problem uses Euclidean (imaginary-time) instanton calculations, which rely on an analogy with the tunneling of a particle through a barrier. However, this approach leaves many questions unanswered—in particular, how does vacuum decay proceed in real time? And what happens in situations where the symmetries of the instanton solutions are broken, e.g., when multiple bubbles are nucleated [14]?

Recently, it has been realized that these questions can be tackled empirically using *quantum analogue experiments* that simulate vacuum decay [15–26]. The original proposal, due to Fialko *et al.* [16, 17], is to create an atomic Bose-Einstein condensate in which two hyperfine states of the same isotope are coupled by a modulated radio-frequency field. Under appropriate conditions, this system is analogous to a relativistic scalar field in a false-vacuum potential, both in terms of its classical equations of motion [18, 20] and its quantum fluctuations [26]. This raises the possibility of carrying out controlled tests of early-Universe theories on a tabletop, allowing us to probe the real-time dynamics of vacuum decay. These hopes are reinforced by recent successes in using cold-atom experiments to study discontinuous phase transitions in quantum fields [27–32], including nonrelativistic thermal vacuum decay [33].

To date this analogy has only been rigorously demonstrated in the ‘symmetric’ case where both states have the same density and *s*-wave scattering length, with zero scattering between the two states. This is challenging

to realize in practice. While the scattering lengths can be tuned using Feshbach resonances in an applied magnetic field [34], this does not provide enough freedom to simultaneously satisfy all of the ‘symmetric’ conditions. As a result, there is only a small, discrete set of options where these conditions hold (and even then, only approximately) [16, 17, 26], leaving little or no flexibility to accommodate other experimental requirements.

Here we relax these conditions, and show that in principle *any* stable mixture between two states of a bosonic isotope can be used to simulate relativistic vacuum decay. This greatly expands the set of possible experimental setups, and will thus accelerate the development of cold-atom simulators of vacuum decay.

Analogue system.—We consider a weakly-interacting Bose gas consisting of two components (‘ \downarrow ’ and ‘ \uparrow ’), which correspond to two states of some bosonic isotope. At low temperatures, each component forms a Bose-Einstein condensate described by a nonrelativistic quantum field $\psi_i(\mathbf{x}) = \sqrt{\hat{n}_i(\mathbf{x})} \exp(i\hat{\phi}_i(\mathbf{x}))$ ($i = \downarrow, \uparrow$), whose modulus $\hat{n}_i(\mathbf{x})$ measures the density of atoms in state i , and whose phase $\hat{\phi}_i(\mathbf{x})$ captures coherent wavelike behavior and interference effects. It is convenient to define the mean density and the population imbalance,

$$n = \frac{\langle \hat{n}_\downarrow \rangle + \langle \hat{n}_\uparrow \rangle}{2}, \quad z = \frac{\langle \hat{n}_\downarrow \rangle - \langle \hat{n}_\uparrow \rangle}{\langle \hat{n}_\downarrow \rangle + \langle \hat{n}_\uparrow \rangle}, \quad (1)$$

which we take as homogeneous throughout the system. In general, the external potential that traps the atoms will give rise to inhomogeneous density profiles for each species—however, we assume the atoms are confined in an optical box trap [35, 36], such that the condensate is homogeneous everywhere except for a small region near to the walls of the trap.

The two species are coupled by a monochromatic

electromagnetic field of frequency $\omega = \omega_0 + \delta$, where $\omega_0 = (E_\uparrow - E_\downarrow)/\hbar$ is the resonant frequency and δ is the detuning. This causes atoms to transition between the two states at a rate Ω set by the amplitude of the coupling, which in general is a function of time. The resulting Hamiltonian is

$$\begin{aligned} \hat{H}(t) = \int_V d\mathbf{x} \left\{ -\hat{\psi}_\downarrow^\dagger \frac{\hbar^2 \nabla^2}{2m} \hat{\psi}_\downarrow - \hat{\psi}_\uparrow^\dagger \frac{\hbar^2 \nabla^2}{2m} \hat{\psi}_\uparrow \right. \\ \left. - \mu(\hat{\psi}_\downarrow^\dagger \hat{\psi}_\downarrow + \hat{\psi}_\uparrow^\dagger \hat{\psi}_\uparrow) - \frac{\hbar \Omega(t)}{2} (\hat{\psi}_\downarrow^\dagger \hat{\psi}_\uparrow + \hat{\psi}_\uparrow^\dagger \hat{\psi}_\downarrow) \right. \\ \left. - \frac{\hbar \delta}{2} (\hat{\psi}_\downarrow^\dagger \hat{\psi}_\downarrow - \hat{\psi}_\uparrow^\dagger \hat{\psi}_\uparrow) + \sum_{i,j} g_{ij} \hat{\psi}_i^\dagger \hat{\psi}_j^\dagger \hat{\psi}_i \hat{\psi}_j \right\}, \end{aligned} \quad (2)$$

where m is the atomic mass, μ is the chemical potential [37], and g_{ij} describes the strength of contact interactions between species i and j , which we parameterize as

$$g = \frac{g_{\downarrow\downarrow} + g_{\uparrow\uparrow}}{2}, \quad \Delta = \frac{g_{\uparrow\uparrow} - g_{\downarrow\downarrow}}{2}, \quad \kappa = \frac{g_{\downarrow\downarrow} + g_{\uparrow\uparrow} - 2g_{\downarrow\uparrow}}{2}. \quad (3)$$

We require repulsive self-interactions ($g_{\downarrow\downarrow}, g_{\uparrow\uparrow} > 0$), while the cross-interaction $g_{\downarrow\uparrow}$ is allowed to have either sign. The condition for miscibility (i.e., existence of a stable homogeneous mean-field) is $g_{\downarrow\downarrow}g_{\uparrow\uparrow} > g_{\downarrow\uparrow}^2$ [38], or equivalently $g^2 - \Delta^2 > (g - \kappa)^2$.

To recover a false-vacuum potential, it is essential that the Rabi coupling consists of a constant piece and an oscillatory piece. The constant piece generates a cosine potential for the relative phase (see Fig. 1), due to the resulting energy cost of putting the species out of phase with each other. This does not allow for vacuum decay, as the state $\varphi = \pi\varphi_0$ is unstable rather than metastable. As pointed out by Fialko *et al.* [16] however, this state can be made metastable by modulating the Rabi coupling. This generates an effective potential barrier, allowing for first-order transitions out of the false vacuum, as illustrated in Fig. 2.

We therefore write the Rabi coupling as [39]

$$\hbar \Omega(t) = 2\epsilon \kappa n \sqrt{1 - z^2} + \lambda \hbar \nu \sqrt{2\epsilon} \cos \nu t, \quad (4)$$

where $\nu \gg \kappa n/\hbar$ is the modulation frequency, and ϵ and λ are dimensionless parameters controlling the amplitudes of the constant and oscillatory terms. Inserting this into Eq. (2), we can use the formalism of Ref. [40] to calculate an effective Hamiltonian, valid for $\epsilon \ll 1$ and on timescales much longer than $2\pi/\nu$ [41]. The false-vacuum potential barrier shown in Fig. 1 is generated by quadratic terms of order ϵ . The constant part of the coupling must also carry a factor of ϵ to ensure that the energy difference between the true and false vacua is of the same order of magnitude as the height of the potential barrier; the exact relationship between the two is set by the $\mathcal{O}(1)$ parameter λ , where $\lambda \geq 1$ is required for metastability, and larger values give longer-lived false vacua.

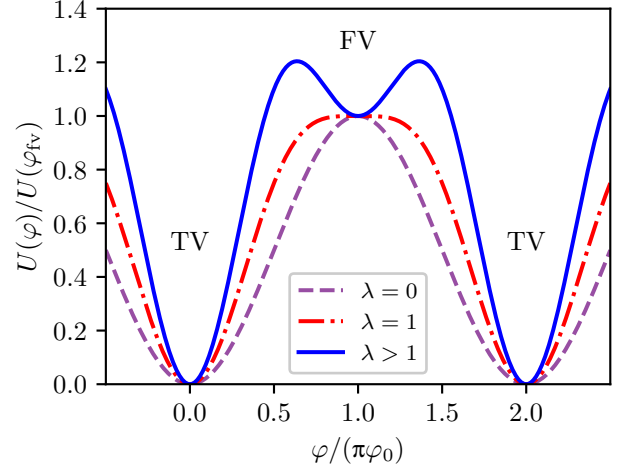


Figure 1. Potential for the pseudorelativistic field φ , as given by Eq. (8). There are stable ‘true vacuum’ (TV) states at even integer values of $\varphi/(\pi\varphi_0)$. For $\lambda > 1$ there are also metastable ‘false vacuum’ (FV) states for odd integer values.

Effective relativistic theory.—Our key result concerns the dynamics of the two phase fields $\hat{\phi}_i(\mathbf{x})$ in the system described above, which are conveniently analyzed in terms of the linear combinations

$$\begin{aligned} \hat{\vartheta}(\mathbf{x}) &= \sqrt{\frac{\hbar^2 n}{2m}} \left((1+z)\hat{\phi}_\downarrow(\mathbf{x}) + (1-z)\hat{\phi}_\uparrow(\mathbf{x}) \right), \\ \hat{\varphi}(\mathbf{x}) &= \sqrt{\frac{\hbar^2 n}{2m}} \sqrt{1-z^2} (\hat{\phi}_\downarrow(\mathbf{x}) - \hat{\phi}_\uparrow(\mathbf{x})). \end{aligned} \quad (5)$$

In situations where density fluctuations $n_i - \langle n_i \rangle$, field gradients $\nabla^2 \vartheta$, $\nabla^2 \varphi$, and the detuning δ are all $\mathcal{O}(\epsilon)$, we can eliminate the densities to obtain a coupled set of equations for the phase fields [41]. For the appropriate population imbalance,

$$z = \frac{\Delta}{\kappa} + \mathcal{O}(\epsilon), \quad (6)$$

these equations decouple to give

$$\begin{aligned} 0 &= (c_\vartheta^{-2} \partial_t^2 - \nabla^2) \vartheta, \\ 0 &= (c_\varphi^{-2} \partial_t^2 - \nabla^2) \varphi + U'(\varphi). \end{aligned} \quad (7)$$

These are the *relativistic* equations of motion for a massless scalar field ϑ and a self-interacting scalar φ in a potential

$$U(\varphi) = m_0^2 \varphi_0^2 \frac{c_\varphi^2}{\hbar^2} \left[1 - \cos(\varphi/\varphi_0) + \frac{\lambda^2}{2} \sin^2(\varphi/\varphi_0) \right], \quad (8)$$

with characteristic mass $m_0 = m \sqrt{4\epsilon \kappa^2 / (\kappa^2 - \Delta^2)}$ and field value $\varphi_0 = \sqrt{(1-z^2)\hbar^2 n / (2m)}$. This potential, as shown in Fig. 1, contains a series of true vacua at $\varphi_{\text{TV}}/\varphi_0 = 2i\pi$, $i \in \mathbb{Z}$, and, for $\lambda > 1$, a series of false vacua at $\varphi_{\text{FV}}/\varphi_0 = (2i+1)\pi$, allowing us to simulate vacuum

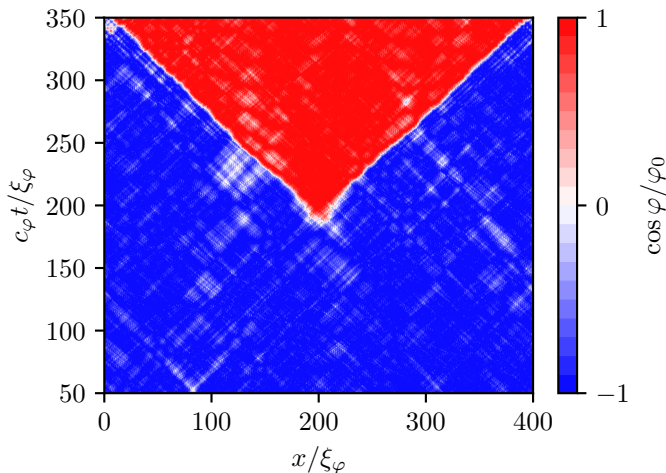


Figure 2. Analogue vacuum decay in a lattice simulation of a 1D potassium-39 analogue system. The metastable ‘false vacuum’ state (blue) spontaneously decays by nucleating a bubble of ‘true vacuum’ (red), which expands until it fills the volume. The pseudorelativistic nature of the system is visible in the ‘lightcone’ shape of the bubble interior.

decay by preparing the system in one of the false vacua. The decoupling is crucial in order to simulate a relativistic system, as the general coupled set of equations cannot be derived from a relativistic Lagrangian.

The two fields (5) each live on a Minkowski spacetime with its own ‘speed of light’ (in reality, the sound speed for the corresponding phonons),

$$c_\vartheta^2 = \frac{n}{m} \left(2g - \kappa - \frac{\Delta^2}{\kappa} \right), \quad c_\varphi^2 = \frac{n}{m} \left(\kappa - \frac{\Delta^2}{\kappa} \right), \quad (9)$$

where $c_\varphi^2 \geq c_\vartheta^2 > 0$ for any miscible system. These define two healing lengths, $\xi_i = \hbar/(\sqrt{2}mc_i)$, which set the length-scale below which nonrelativistic effects become important in each field, thus determining the regime of validity of the relativistic analogy.

This ‘bi-metric’ structure for phonons in Bose-Bose mixtures was previously studied in Refs. [42–44], where a decoupling condition analogous to Eq. (6) was derived for linearized perturbations around a fixed background in the case $g_{\downarrow\uparrow} = 0$. Here we generalize the decoupling to any $g_{\downarrow\uparrow}$, which greatly broadens the range of corresponding cold-atom systems, and derive a fully nonlinear relativistic theory for the phase fields, which is crucial for simulating the nonperturbative dynamics of vacuum decay.

One can show that our decoupling condition (6) is equivalent to equating the chemical potentials of the two species, $\mu_\downarrow = \mu_\uparrow$. This makes intuitive sense, as each chemical potential sets the average rate at which the corresponding phase evolves over time. This equality therefore ensures that the relative phase has zero mean velocity, as expected for the relativistic field φ . Equating the two chemical potentials also suppresses fluctuations

in the density degrees of freedom, which is an essential requirement for pseudorelativistic phase dynamics.

As well as the classical, nonlinear equations of motion (7), we have verified that the relativistic analogy holds at the level of the vacuum fluctuations, which is crucial for faithfully simulating the decay rate [26]. Expanding the Hamiltonian to quadratic order in the fluctuations, we find that it decouples into two independent sectors *if and only if* Eq. (6) holds. Diagonalizing each sector with a Bogoliubov transformation, we find that on scales much larger than their respective healing lengths ($\xi_i k \ll 1$) the dispersion relations of the two fields match the expressions for a massless relativistic scalar ϑ and a self-interacting scalar φ with the false-vacuum potential given in Eq. (8), and with the sound speeds given by Eq. (9). This nontrivial check confirms all of the key details of the effective relativistic theory described above.

Experimental proposal.—Our results open an extensive new landscape of possibilities for analogue vacuum decay. As an illustrative example, we present a feasible set of parameters for an asymmetric homonuclear mixture in potassium-39 (^{39}K). We consider the hyperfine states $|\downarrow\rangle \equiv |F=1, m_F=0\rangle$ and $|\uparrow\rangle \equiv |F=1, m_F=-1\rangle$ (with F and m_F the total and projected angular momenta), which are miscible in an external magnetic field $B \approx 57\text{--}59\text{ G}$. Mixtures of these states have been used extensively in studies of ‘quantum droplet’ formation just outside of the miscible regime [45–48].

While our results are valid in any number of dimensions, we focus here on a quasi-1D experiment in which the atoms are tightly confined along the two transverse directions. This offers several practical advantages, including the option of carrying out many runs simultaneously with an array of 1D traps, or eliminating the box trap boundary conditions by using a 1D ring. The decay rate is also parametrically faster in 1D than in higher dimensions [41], allowing us to probe a broader range of parameter space within the $\sim 1\text{ s}$ coherence time of each run. A 2D setup is also possible, and would allow us to investigate a greater range of physical phenomena, such as domain walls between topologically distinct true vacua. A 3D setup would carry further technical complications associated with simultaneously levitating both species against gravity [36].

Our proposed experimental parameters are summarized in Table I. These were chosen to maximize the characteristic energy scale of the condensate, as this suppresses the influence of thermal fluctuations for a fixed temperature. This results in a significant population imbalance, $z \sim 0.7$, which differs strongly from the symmetric case $z = 0$. To scan over a range of decay rates, we vary the number of atoms and the strength of the transverse trap inversely to each other, holding the 1D energy scale constant. This allows us to vary the dimensionless number density $\bar{n}_\varphi = \xi_\varphi n$, which controls the relative size of vacuum fluctuations, while leaving all other paramet-

Parameter	Value
Atomic isotope	potassium-39 (^{39}K)
Atomic mass	$m = 38.96 \text{ u} = 6.470 \times 10^{-26} \text{ kg}$
Hyperfine states	$ \downarrow\rangle \equiv F=1, m_F=0\rangle$ $ \uparrow\rangle \equiv F=1, m_F=-1\rangle$
Magnetic field	$B = 58.50 \text{ G}$
Scattering lengths (3D)	$a_{\downarrow\downarrow} = 31.85 a_0 = 1.686 \text{ nm}$ $a_{\uparrow\uparrow} = 446.2 a_0 = 23.61 \text{ nm}$ $a_{\downarrow\uparrow} = -51.84 a_0 = -2.743 \text{ nm}$
Population imbalance	$z = 0.7159$
Imaging efficiency	$\sqrt{1-z^2} = 0.6982$
Healing lengths	$\xi_\vartheta = 1.797 \times 10^4 a_0 = 1.141 \mu\text{m}$ $\xi_\varphi = 9.449 \times 10^3 a_0 = 0.600 \mu\text{m}$
Sound speeds	$c_\vartheta = 1.010 \text{ mm s}^{-1}$ $c_\varphi = 1.921 \text{ mm s}^{-1}$
Energy scales	$mc_\vartheta^2 = 0.412 \text{ peV} = 4.78 k_B \text{ nK}$ $mc_\varphi^2 = 1.490 \text{ peV} = 17.29 k_B \text{ nK}$
Box trap length	$L = 400 \xi_\varphi = 240 \mu\text{m}$
Sound-crossing time	$L/c_\varphi = 124.9 \text{ ms}$
Total number of atoms	$8000 \leq N \leq 32000$
Density per species	$16.67 \mu\text{m}^{-1} \leq n \leq 66.67 \mu\text{m}^{-1}$
Dimensionless density	$10 \leq \bar{n}_\varphi \leq 40$
Transverse trap frequency	$0.356 \text{ kHz} \leq \omega_\perp/2\pi \leq 1.43 \text{ kHz}$
Mean Rabi frequency	$\Omega_0 = 16.04 \text{ Hz}$
Rabi coupling parameter	$\epsilon = 2.5 \times 10^{-3}$
Modulation amplitude	$\lambda = \sqrt{2}$
False vacuum mass	$m_{\text{fv}} = \sqrt{\lambda^2 - 1} m_0 = 0.1425 m$

Table I. List of parameters for our proposed 1D experiment. Here $\text{u} = 1.661 \times 10^{-27} \text{ kg}$ and $a_0 = 5.292 \times 10^{-2} \text{ nm}$. The dimensionless density $\bar{n}_\varphi = \xi_\varphi n$ (which sets the decay rate) is scanned over by varying the total number of atoms N and the frequency of the transverse harmonic trap ω_\perp .

ers of the relativistic theory fixed [26]. Since the decay rate scales like $\log \Gamma \sim -\bar{n}_\varphi$, even the small range of \bar{n}_φ considered here is enough to probe a broad range of scenarios.

It is straightforward to prepare the false vacuum state by applying a strong, far-detuned radio-frequency field to a pure- $|\downarrow\rangle$ or pure- $|\uparrow\rangle$ condensate, adiabatically varying the detuning until the desired population imbalance is achieved [41]. After allowing the system to evolve for some time, the relative phase is then imaged by using a radio-frequency pulse to convert it into a density contrast between true- and false-vacuum regions. This contrast is imaged with an efficiency of $\sqrt{1-z^2}$, which is $\sim 70\%$ for our example system. Analyzing these snapshots over many runs then allows one to extract interesting physical quantities such as the decay rate.

Lattice simulations.—We test our predictions with semiclassical lattice simulations, using the full time-dependent Hamiltonian (2) to evolve the atomic fields

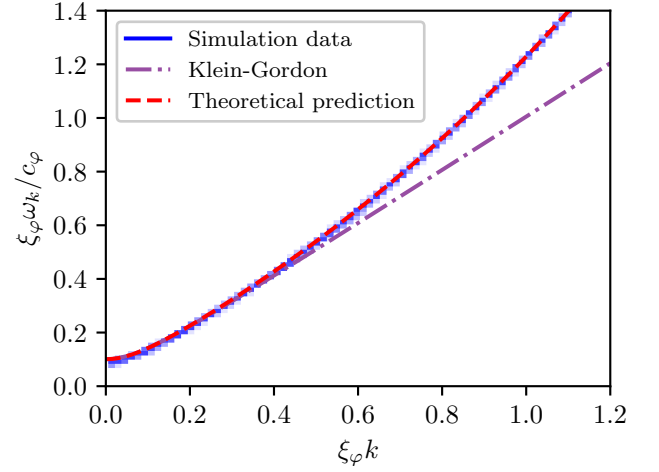


Figure 3. Dispersion relationship for the relative phase φ around the false vacuum $\langle\varphi\rangle = \pi\varphi_0$. The blue heatmap shows the averaged result from 32 independent simulations of the system described in Table I (with $\bar{n}_\varphi = 100$, so that no bubble nucleation occurs). This dispersion relationship interpolates between that of a Klein Gordon field of mass m_{fv} on large scales and that of a nonrelativistic Schrödinger field on small scales, and agrees with our theoretical prediction (red).

ψ_i . These simulations capture the nonclassical nature of the system by including vacuum fluctuations in the initial conditions. The fields are then evolved forward in real time by numerically integrating the classical equations of motion. By repeating this for an ensemble of initial conditions, we obtain a semiclassical approximation to the behavior of the system, commonly referred to as the ‘truncated Wigner approximation’ [49].

We simulate a ^{39}K mixture in a periodic 1D box, using the parameters in Table I. In each simulation, we set z by minimizing the chemical potential of the homogeneous false vacuum, with zero detuning. This corresponds to the critical value in Eq. (6), including an $\mathcal{O}(\epsilon)$ correction that we obtain explicitly. We then draw randomized vacuum fluctuations in the ϑ and φ fields and their conjugate momenta, and use our chosen value of z to convert these into fluctuations in the ψ_i fields.

We have carried out several consistency checks with our simulations [41], all of which confirm that ϑ and φ behave like decoupled relativistic fields *if and only if* Eq. (6) holds. One such check is shown in Fig. 3, where we see that the dispersion relationship for φ measured in our simulations exhibits excellent agreement with our theoretical prediction, including pseudorelativistic behavior on scales much larger than the healing length ξ_φ .

These checks are all carried out for large dimensionless densities, $\bar{n}_\varphi \geq 100$. This suppresses the vacuum fluctuations, so that our perturbative calculations give a good approximation to the dynamics of the system. For the lower densities that are experimentally accessible with this setup, $\bar{n}_\varphi \lesssim 40$, one expects backreaction from the fluctu-

ations to become significant, leading to deviations from our predictions. In particular, this will give corrections to the critical z , so that the simple expression in Eq. (6) no longer gives a long-lived metastable state. We verify this numerically, finding that simulations with $\bar{n}_\varphi \lesssim 40$ decay rapidly due to a homogeneous initial velocity in the φ field that carries it over the potential barrier.

In principle one should account for backreaction analytically, calculating the renormalized critical value of z . We find that a simpler solution is to introduce a small detuning that compensates for the error in z , such that the initial mean velocity of φ vanishes. Using this prescription, we find that our simulations exhibit precisely the expected behavior, passing all of the same consistency checks as before. This procedure could be implemented experimentally using ensembles of runs with different detuning values, selecting the value that maximizes the lifetime of the metastable state.

Summary and outlook.—Cold-atom analogue experiments will soon provide the first empirical tests of vacuum decay. We have shown that the landscape of suitable analogues is much larger than previously thought, demonstrating that *any* stable homonuclear Bose-Bose mixture can be used to simulate relativistic quantum fields. These experiments have enormous discovery potential, allowing us to test predictions for the decay rate (potentially resolving or confirming the discrepancy between instanton predictions and lattice simulations [50, 51]), as well as probing physics beyond the reach of instanton calculations, such as bubble-bubble correlations [14], with a broad range of possible implications for the physics of the early Universe.

Acknowledgments.—We thank Jonathan Braden, Christoph Eigen, Matthew Johnson, Konstantinos Konstantinou, Dalila Pirvu, Tanish Satoor, Silke Weinfurter, and Paul Wong for valuable discussions. This work was supported by the Science and Technology Facilities Council (STFC) [grants ST/T000708/1 and ST/T006056/1], the UK Quantum Technologies for Fundamental Physics programme [grants ST/T005904/1, ST/T00584X/1, and ST/W006162/1], and the European Research Council (ERC) [UniFlat], and was partly enabled by the UCL Cosmoparticle Initiative. ZH acknowledges support from the Royal Society Wolfson Fellowship. This research was supported in part by Perimeter Institute for Theoretical Physics. Research at Perimeter Institute is supported in part by the Government of Canada through the Department of Innovation, Science and Economic Development Canada and by the Province of Ontario through the Ministry of Colleges and Universities. We acknowledge the use of the Python packages NumPy [52], SciPy [53], and Matplotlib [54]. The data that support the findings of this study are available from the corresponding author, ACJ, under reasonable request.

Author contributions.—Based on the CRediT (Contribution Roles Taxonomy) system. **ACJ**: methodology;

software; formal analysis; investigation; data curation; interpretation and validation; visualization; writing (original draft). **IGM**: methodology; formal analysis; investigation; interpretation and validation; writing (review). **TPB**: methodology; interpretation and validation; writing (review). **ZH**: conceptualization; interpretation and validation; writing (review). **HVP**: interpretation and validation; writing (review); project administration. **AP**: interpretation and validation; writing (review).

* alex.jenkins@ucl.ac.uk

- [1] Sidney R. Coleman, “The Fate of the False Vacuum. 1. Semiclassical Theory,” *Phys. Rev. D* **15**, 2929–2936 (1977), [Erratum: *Phys. Rev. D* 16, 1248(E) (1977)].
- [2] Curtis G. Callan, Jr. and Sidney R. Coleman, “The Fate of the False Vacuum. 2. First Quantum Corrections,” *Phys. Rev. D* **16**, 1762–1768 (1977).
- [3] Sidney R. Coleman and Frank De Luccia, “Gravitational Effects on and of Vacuum Decay,” *Phys. Rev. D* **21**, 3305 (1980).
- [4] Andrei D. Linde, “Decay of the False Vacuum at Finite Temperature,” *Nucl. Phys. B* **216**, 421 (1983), [Erratum: *Nucl. Phys. B* 223, 544 (1983)].
- [5] Erick J. Weinberg, *Classical solutions in quantum field theory: Solitons and Instantons in High Energy Physics*, Cambridge Monographs on Mathematical Physics (Cambridge University Press, 2012).
- [6] Alan H. Guth, “Eternal inflation and its implications,” *J. Phys. A* **40**, 6811–6826 (2007), [arXiv:hep-th/0702178](https://arxiv.org/abs/hep-th/0702178).
- [7] Anthony Aguirre, “Eternal Inflation, past and future,” (2007), [arXiv:0712.0571](https://arxiv.org/abs/0712.0571) [hep-th].
- [8] Anthony Aguirre, Matthew C. Johnson, and Asaf Shomer, “Towards observable signatures of other bubble universes,” *Phys. Rev. D* **76**, 063509 (2007), [arXiv:0704.3473](https://arxiv.org/abs/0704.3473) [hep-th].
- [9] Stephen M. Feeney, Matthew C. Johnson, Daniel J. Mortlock, and Hiranya V. Peiris, “First Observational Tests of Eternal Inflation,” *Phys. Rev. Lett.* **107**, 071301 (2011), [arXiv:1012.1995](https://arxiv.org/abs/1012.1995) [astro-ph.CO].
- [10] Stephen M. Feeney, Matthew C. Johnson, Daniel J. Mortlock, and Hiranya V. Peiris, “First Observational Tests of Eternal Inflation: Analysis Methods and WMAP 7-Year Results,” *Phys. Rev. D* **84**, 043507 (2011), [arXiv:1012.3667](https://arxiv.org/abs/1012.3667) [astro-ph.CO].
- [11] J. Ellis, J. R. Espinosa, G. F. Giudice, A. Hoecker, and A. Riotto, “The Probable Fate of the Standard Model,” *Phys. Lett. B* **679**, 369–375 (2009), [arXiv:0906.0954](https://arxiv.org/abs/0906.0954) [hep-ph].
- [12] Giuseppe Degrandi, Stefano Di Vita, Joan Elias-Miro, Jose R. Espinosa, Gian F. Giudice, Gino Isidori, and Alessandro Strumia, “Higgs mass and vacuum stability in the Standard Model at NNLO,” *JHEP* **08**, 098 (2012), [arXiv:1205.6497](https://arxiv.org/abs/1205.6497) [hep-ph].
- [13] Dario Buttazzo, Giuseppe Degrandi, Pier Paolo Giardinò, Gian F. Giudice, Filippo Sala, Alberto Salvio, and Alessandro Strumia, “Investigating the near-criticality of the Higgs boson,” *JHEP* **12**, 089 (2013), [arXiv:1307.3536](https://arxiv.org/abs/1307.3536) [hep-ph].
- [14] Dalila Pirvu, Jonathan Braden, and Matthew C. Johnson

- son, “Bubble clustering in cosmological first order phase transitions,” *Phys. Rev. D* **105**, 043510 (2022), [arXiv:2109.04496 \[hep-th\]](#).
- [15] Bogdan Opanchuk, Rodney Polkinghorne, Oleksandr Fialko, Joachim Brand, and Peter D. Drummond, “Quantum simulations of the early universe,” *Annalen Phys.* **525**, 866–876 (2013), [arXiv:1305.5314 \[cond-mat.quant-gas\]](#).
- [16] O. Fialko, B. Opanchuk, A. I. Sidorov, P. D. Drummond, and J. Brand, “Fate of the false vacuum: towards realization with ultra-cold atoms,” *EPL* **110**, 56001 (2015), [arXiv:1408.1163 \[cond-mat.quant-gas\]](#).
- [17] Oleksandr Fialko, Bogdan Opanchuk, Andrei I. Sidorov, Peter D. Drummond, and Joachim Brand, “The universe on a table top: engineering quantum decay of a relativistic scalar field from a metastable vacuum,” *J. Phys. B* **50**, 024003 (2017), [arXiv:1607.01460 \[cond-mat.quant-gas\]](#).
- [18] Jonathan Braden, Matthew C. Johnson, Hiranya V. Peiris, and Silke Weinfurter, “Towards the cold atom analog false vacuum,” *JHEP* **07**, 014 (2018), [arXiv:1712.02356 \[hep-th\]](#).
- [19] Thomas P. Billam, Ruth Gregory, Florent Michel, and Ian G. Moss, “Simulating seeded vacuum decay in a cold atom system,” *Phys. Rev. D* **100**, 065016 (2019), [arXiv:1811.09169 \[hep-th\]](#).
- [20] Jonathan Braden, Matthew C. Johnson, Hiranya V. Peiris, Andrew Pontzen, and Silke Weinfurter, “Nonlinear Dynamics of the Cold Atom Analog False Vacuum,” *JHEP* **10**, 174 (2019), [arXiv:1904.07873 \[hep-th\]](#).
- [21] Thomas P. Billam, Kate Brown, and Ian G. Moss, “Simulating cosmological supercooling with a cold atom system,” *Phys. Rev. A* **102**, 043324 (2020), [arXiv:2006.09820 \[cond-mat.quant-gas\]](#).
- [22] King Lun Ng, Bogdan Opanchuk, Manushan Thenabadu, Margaret Reid, and Peter D. Drummond, “The fate of the false vacuum: Finite temperature, entropy and topological phase in quantum simulations of the early universe,” *PRX Quantum* **2**, 010350 (2021), [arXiv:2010.08665 \[quant-ph\]](#).
- [23] Thomas P. Billam, Kate Brown, Andrew J. Groszek, and Ian G. Moss, “Simulating cosmological supercooling with a cold atom system. II. Thermal damping and parametric instability,” *Phys. Rev. A* **104**, 053309 (2021), [arXiv:2104.07428 \[cond-mat.quant-gas\]](#).
- [24] Thomas P. Billam, Kate Brown, and Ian G. Moss, “False-vacuum decay in an ultracold spin-1 Bose gas,” *Phys. Rev. A* **105**, L041301 (2022), [arXiv:2108.05740 \[cond-mat.quant-gas\]](#).
- [25] Thomas P. Billam, Kate Brown, and Ian G. Moss, “Bubble nucleation in a cold spin 1 gas,” *New J. Phys.* **25**, 043028 (2023), [arXiv:2212.03621 \[cond-mat.quant-gas\]](#).
- [26] Alexander C. Jenkins, Jonathan Braden, Hiranya V. Peiris, Andrew Pontzen, Matthew C. Johnson, and Silke Weinfurter, “From the tabletop to the Big Bang: Analogue vacuum decay from vacuum initial conditions,” (2023), [arXiv:2307.02549 \[cond-mat.quant-gas\]](#).
- [27] J. Struck, M. Weinberg, C. Ölschläger, P. Windpassinger, J. Simonet, K. Sengstock, R. Höppner, P. Hauke, A. Eckardt, M. Lewenstein, and L. Mathey, “Engineering Ising-XY spin-models in a triangular lattice using tunable artificial gauge fields,” *Nature Phys.* **9**, 738–743 (2013), [arXiv:1304.5520 \[cond-mat.quant-gas\]](#).
- [28] D. L. Campbell, R. M. Price, A. Putra, A. Valdés-Curiel, D. Trypogeorgos, and I. B. Spielman, “Magnetic phases of spin-1 spin-orbit-coupled Bose gases,” *Nature Communications* **7**, 10897 (2016), [arXiv:1501.05984 \[cond-mat.quant-gas\]](#).
- [29] A. Trenkwalder, G. Spagnolli, G. Semeghini, S. Coop, M. Landini, P. Castilho, L. Pezzè, G. Modugno, M. Inguscio, A. Smerzi, and M. Fattori, “Quantum phase transitions with parity-symmetry breaking and hysteresis,” *Nature Phys.* **12**, 826–829 (2016), [arXiv:1603.02979 \[cond-mat.quant-gas\]](#).
- [30] L.-Y. Qiu, H.-Y. Liang, Y.-B. Yang, H.-X. Yang, T. Tian, Y. Xu, and L.-M. Duan, “Observation of generalized Kibble-Zurek mechanism across a first-order quantum phase transition in a spinor condensate,” *Science Advances* **6**, eaba7292 (2020), [arXiv:2001.10210 \[cond-mat.quant-gas\]](#).
- [31] Bo Song, Shovan Dutta, Shaurya Bhawe, Jr-Chiun Yu, Edward Carter, Nigel Cooper, and Ulrich Schneider, “Realizing discontinuous quantum phase transitions in a strongly correlated driven optical lattice,” *Nature Phys.* **18**, 259–264 (2022), [arXiv:2105.12146 \[cond-mat.quant-gas\]](#).
- [32] Riccardo Cominotti, Anna Berti, Clement Dulin, Chiara Rogora, Giacomo Lamporesi, Iacopo Carusotto, Alessio Recati, Alessandro Zenesini, and Gabriele Ferrari, “Ferromagnetism in an Extended Coherently Coupled Atomic Superfluid,” *Phys. Rev. X* **13**, 021037 (2023), [arXiv:2209.13235 \[cond-mat.quant-gas\]](#).
- [33] Alessandro Zenesini, Anna Berti, Riccardo Cominotti, Chiara Rogora, Ian G. Moss, Thomas P. Billam, Iacopo Carusotto, Giacomo Lamporesi, Alessio Recati, and Gabriele Ferrari, “Observation of false vacuum decay via bubble formation in ferromagnetic superfluids,” (2023), [arXiv:2305.05225 \[hep-ph\]](#).
- [34] Cheng Chin, Rudolf Grimm, Paul Julienne, and Eite Tiesinga, “Feshbach resonances in ultracold gases,” *Rev. Mod. Phys.* **82**, 1225–1286 (2010), [arXiv:0812.1496 \[cond-mat.other\]](#).
- [35] Alexander L. Gaunt, Tobias F. Schmidutz, Igor Gotlibovych, Robert P. Smith, and Zoran Hadzibabic, “Bose-Einstein Condensation of Atoms in a Uniform Potential,” *Phys. Rev. Lett.* **110**, 200406 (2013), [arXiv:1212.4453 \[cond-mat.quant-gas\]](#).
- [36] Nir Navon, Robert P. Smith, and Zoran Hadzibabic, “Quantum gases in optical boxes,” *Nature Phys.* **17**, 1334–1341 (2021), [arXiv:2106.09716 \[cond-mat.quant-gas\]](#).
- [37] This is the chemical potential for the total number $N = N_{\downarrow} + N_{\uparrow}$, and should thus be interpreted as the energy cost associated with adding atoms of both species to the system at constant z . This is distinguished from the individual chemical potentials μ_{\downarrow} , μ_{\uparrow} , which correspond to adding atoms of a single species to the system. (‘Chemical potential’ here simply means the partial derivative of energy with respect to particle number, and thus does not require chemical equilibrium.).
- [38] C. J. Pethick and H. Smith, *Bose-Einstein Condensation in Dilute Gases*, 2nd ed. (Cambridge University Press, 2008).
- [39] Note that we allow this expression to become negative, so that the phase as well as the amplitude of the Rabi coupling are modulated.
- [40] N. Goldman and J. Dalibard, “Periodically-driven quantum systems: Effective Hamiltonians and engineered gauge fields,” *Phys. Rev. X* **4**, 031027 (2014), [Erratum: *Phys. Rev. X* **5**, 029902(E) (2015)], [arXiv:1404.4373 \[cond-mat.quant-gas\]](#).

- [41] See Supplemental Material for further details regarding: the time-averaged Hamiltonian; the identification of the true and false vacuum states; the derivation of the relativistic equations of motion; the vacuum fluctuation statistics in the false vacuum; the Euclidean bounce action for our effective relativistic theory; the state initialization protocol; and our lattice simulations.
- [42] Matt Visser and Silke Weinfurtnr, “Massive phonon modes from a BEC-based analog model,” (2004), [arXiv:cond-mat/0409639](#).
- [43] Matt Visser and Silke Weinfurtnr, “Massive Klein-Gordon equation from a BEC-based analogue spacetime,” *Phys. Rev. D* **72**, 044020 (2005), [arXiv:gr-qc/0506029](#).
- [44] Silke Weinfurtnr, Stefano Liberati, and Matt Visser, “Analogue spacetime based on 2-component Bose-Einstein condensates,” *Lect. Notes Phys.* **718**, 115–163 (2007), [arXiv:gr-qc/0605121](#).
- [45] C. R. Cabrera, L. Tanzi, J. Sanz, B. Naylor, P. Thomas, P. Cheiney, and L. Tarruell, “Quantum liquid droplets in a mixture of Bose-Einstein condensates,” *Science* **359**, 301–304 (2018), [arXiv:1708.07806 \[cond-mat.quant-gas\]](#).
- [46] G. Semeghini, G. Ferioli, L. Masi, C. Mazzinghi, L. Wolswijk, F. Minardi, M. Modugno, G. Modugno, M. Inguscio, and M. Fattori, “Self-bound quantum droplets in atomic mixtures,” *Phys. Rev. Lett.* **120**, 235301 (2018), [arXiv:1710.10890 \[cond-mat.quant-gas\]](#).
- [47] P. Cheiney, C. R. Cabrera, J. Sanz, B. Naylor, L. Tanzi, and L. Tarruell, “Bright soliton to quantum droplet transition in a mixture of Bose-Einstein condensates,” *Phys. Rev. Lett.* **120**, 135301 (2018), [arXiv:1710.11079 \[cond-mat.quant-gas\]](#).
- [48] Giovanni Ferioli, Giulia Semeghini, Leonardo Masi, Giovanni Giusti, Giovanni Modugno, Massimo Inguscio, Albert Gallemì, Alessio Recati, and Marco Fattori, “Collisions of self-bound quantum droplets,” *Phys. Rev. Lett.* **122**, 090401 (2019), [arXiv:1812.09151 \[cond-mat.quant-gas\]](#).
- [49] P. B. Blakie, A. S. Bradley, M. J. Davis, R. J. Ballagh, and C. W. Gardiner, “Dynamics and statistical mechanics of ultra-cold Bose gases using c-field techniques,” *Adv. Phys.* **57**, 363 (2008), [arXiv:0809.1487 \[cond-mat.stat-mech\]](#).
- [50] Jonathan Braden, Matthew C. Johnson, Hiranya V. Peiris, Andrew Pontzen, and Silke Weinfurtnr, “New Semiclassical Picture of Vacuum Decay,” *Phys. Rev. Lett.* **123**, 031601 (2019), [Erratum: *Phys. Rev. Lett.* **129**, 059901 (2022)], [arXiv:1806.06069 \[hep-th\]](#).
- [51] Jonathan Braden, Matthew C. Johnson, Hiranya V. Peiris, Andrew Pontzen, and Silke Weinfurtnr, “Mass renormalization in lattice simulations of false vacuum decay,” *Phys. Rev. D* **107**, 083509 (2023), [arXiv:2204.11867 \[hep-th\]](#).
- [52] Charles R. Harris, K. Jarrod Millman, Stéfan J. van der Walt, Ralf Gommers, Pauli Virtanen, David Cournapeau, Eric Wieser, Julian Taylor, Sebastian Berg, Nathaniel J. Smith, Robert Kern, Matti Picus, Stephan Hoyer, Marten H. van Kerkwijk, Matthew Brett, Allan Haldane, Jaime Fernández del Río, Mark Wiebe, Pearu Peterson, Pierre Gérard-Marchant, Kevin Sheppard, Tyler Reddy, Warren Weckesser, Hameer Abbasi, Christoph Gohlke, and Travis E. Oliphant, “Array programming with NumPy,” *Nature* **585**, 357–362 (2020), [arXiv:2006.10256 \[cs.MS\]](#).
- [53] Pauli Virtanen, Ralf Gommers, Travis E. Oliphant, Matt Haberland, Tyler Reddy, David Cournapeau, Evgeni Burovski, Pearu Peterson, Warren Weckesser, Jonathan Bright, Stéfan J. van der Walt, Matthew Brett, Joshua Wilson, K. Jarrod Millman, Nikolay Mayorov, Andrew R. J. Nelson, Eric Jones, Robert Kern, Eric Larson, C. J. Carey, İlhan Polat, Yu Feng, Eric W. Moore, Jake VanderPlas, Denis Laxalde, Josef Perktold, Robert Cimrman, Ian Henriksen, E. A. Quintero, Charles R. Harris, Anne M. Archibald, Antônio H. Ribeiro, Fabian Pedregosa, Paul van Mulbregt, and SciPy 1.0 Contributors, “SciPy 1.0—Fundamental Algorithms for Scientific Computing in Python,” *Nature Meth.* **17**, 261 (2020), [arXiv:1907.10121 \[cs.MS\]](#).
- [54] John D. Hunter, “Matplotlib: A 2D Graphics Environment,” *Comput. Sci. Eng.* **9**, 90–95 (2007).

SUPPLEMENTAL MATERIAL

Time-averaged Hamiltonian

The Hamiltonian for our system can be split into a constant piece and an oscillating perturbation due to the modulation of the Rabi coupling,

$$\begin{aligned}\hat{H}(t) &= \hat{H}_0 - \lambda \hbar \nu \sqrt{2\epsilon} \hat{X} \cos(\nu t), \\ \hat{X} &= \frac{1}{2} \int_V d\mathbf{x} (\hat{\psi}_\downarrow^\dagger \hat{\psi}_\uparrow + \hat{\psi}_\uparrow^\dagger \hat{\psi}_\downarrow).\end{aligned}\quad (10)$$

Using the formalism developed in Ref. [40], we obtain an effective time-averaged Hamiltonian that governs the dynamics of modes with frequencies much less than ν . The small parameter ϵ associated with the amplitude of the Rabi coupling allows us to write this perturbatively as

$$\hat{H}_{\text{eff}} = \hat{H}_0 + \frac{\epsilon \lambda^2}{2} [[\hat{X}, \hat{H}_0], \hat{X}] + \mathcal{O}(\epsilon^2). \quad (11)$$

Evaluating the commutators, this gives (to linear order in ϵ)

$$\begin{aligned}\hat{H}_{\text{eff}} &= \int_V d\mathbf{x} \left\{ -\hat{\psi}_\downarrow^\dagger \frac{\hbar^2 \nabla^2}{2m} \hat{\psi}_\downarrow - \hat{\psi}_\uparrow^\dagger \frac{\hbar^2 \nabla^2}{2m} \hat{\psi}_\uparrow \right. \\ &\quad - \mu (\hat{\psi}_\downarrow^\dagger \hat{\psi}_\downarrow + \hat{\psi}_\uparrow^\dagger \hat{\psi}_\uparrow) - \epsilon \kappa n \sqrt{1-z^2} (\hat{\psi}_\downarrow^\dagger \hat{\psi}_\uparrow + \hat{\psi}_\uparrow^\dagger \hat{\psi}_\downarrow) \\ &\quad - \frac{\hbar \delta}{2} \left(1 - \frac{\epsilon \lambda^2}{2} \right) (\hat{\psi}_\downarrow^\dagger \hat{\psi}_\downarrow - \hat{\psi}_\uparrow^\dagger \hat{\psi}_\uparrow) \\ &\quad + \frac{1}{2} \left(g - \Delta - \frac{\epsilon \lambda^2}{2} (\kappa - \Delta) \right) \hat{\psi}_\downarrow^\dagger \hat{\psi}_\downarrow \hat{\psi}_\downarrow \hat{\psi}_\downarrow \\ &\quad + \frac{1}{2} \left(g + \Delta - \frac{\epsilon \lambda^2}{2} (\kappa + \Delta) \right) \hat{\psi}_\uparrow^\dagger \hat{\psi}_\uparrow \hat{\psi}_\uparrow \hat{\psi}_\uparrow \\ &\quad + (g - \kappa(1 - \epsilon \lambda^2)) \hat{\psi}_\downarrow^\dagger \hat{\psi}_\downarrow \hat{\psi}_\uparrow^\dagger \hat{\psi}_\uparrow \\ &\quad \left. - \frac{\epsilon \lambda^2}{4} \kappa (\hat{\psi}_\downarrow^\dagger \hat{\psi}_\downarrow \hat{\psi}_\uparrow \hat{\psi}_\uparrow + \hat{\psi}_\uparrow^\dagger \hat{\psi}_\uparrow \hat{\psi}_\downarrow \hat{\psi}_\downarrow) \right\}.\end{aligned}\quad (12)$$

As discussed in Refs. [18, 20], this time-averaged analysis neglects the presence of parametric resonances due to the driven coupling, which lead to an instability in modes with frequencies on the order of ν . In the experimental context, one expects to be able to damp this instability by making the driving frequency sufficiently large.

Identifying the false vacuum state

We consider first the dynamics of the zero mode of the system, with the aim of finding stationary mean-field solutions that we will identify with the true and false vacua of the effective relativistic theory. Neglecting inhomogeneities, there are only two dynamical degrees

of freedom: the relative phase φ , and the population imbalance z . (In a homogeneous system the total density n is constant, and the total phase ϑ is pure gauge.) The classical equations of motion under the time-averaged Hamiltonian (12) are

$$\begin{aligned}\dot{\varphi}/\varphi_0 &= -\frac{\Omega_0 z}{\sqrt{1-z^2}} \cos(\varphi/\varphi_0) + (2 - \epsilon \lambda^2) \left(\frac{\Delta n}{\hbar} + \frac{\delta}{2} \right) \\ &\quad - \frac{\kappa n z}{\hbar} [2 + \epsilon \lambda^2 (3 - \cos(2\varphi/\varphi_0))], \\ \frac{\dot{z}}{\sqrt{1-z^2}} &= \frac{\Omega_0}{\sqrt{1-z^2}} \sin(\varphi/\varphi_0) + \epsilon \lambda^2 \frac{\kappa n}{\hbar} \sin(2\varphi/\varphi_0),\end{aligned}\quad (13)$$

where Ω_0 is the constant piece of the Rabi coupling. These equations admit two stationary solutions, which we identify with the true and false vacua of the effective relativistic theory,

$$\varphi/\varphi_0 = 0 \text{ or } \pi, \quad z = \frac{\Delta}{\kappa} + \mathcal{O}(\epsilon), \quad (14)$$

i.e., the two species are either in phase or in antiphase, with a population imbalance matching that in Eq. (6). (The $\mathcal{O}(\epsilon)$ term differs slightly between the two solutions, but as discussed above this correction has little to no effect on the dynamics.)

In Fig. 4 we show phase portraits for the dynamical system defined by Eq. (13), with and without modulation. For modulation of sufficiently large amplitude, $\lambda > 1$, we see that both stationary solutions are classically stable, with small perturbations giving rise to bound orbits. However, the energy of the antiphase state is greater than that of the in-phase state, rendering it metastable once we include vacuum fluctuations. As expected, we also see that the antiphase state becomes unstable if we switch off the modulation.

Relativistic equations of motion

We now consider the full field theory, allowing inhomogeneous modes in the two species, in order to establish the relativistic equations of motion (7). It is convenient to write the atomic fields as

$$\begin{aligned}\psi_\downarrow &= \sqrt{n(1+z)} \exp(f_\downarrow + i\phi_\downarrow), \\ \psi_\uparrow &= \sqrt{n(1-z)} \exp(f_\uparrow + i\phi_\uparrow),\end{aligned}\quad (15)$$

where n and z are constants that define fixed background densities, and f_i are fields encoding deviations from this background. We assume that $f_i \sim \mathcal{O}(\epsilon)$, but do not consider any fixed background values for the phases ϕ_i ; this is crucial to obtain a nonlinear relativistic theory with a false-vacuum potential. Assuming that field gradients and the detuning are small, $\hbar^2 \nabla^2 / (\kappa n m) \sim \hbar \delta / (\kappa n) \sim$

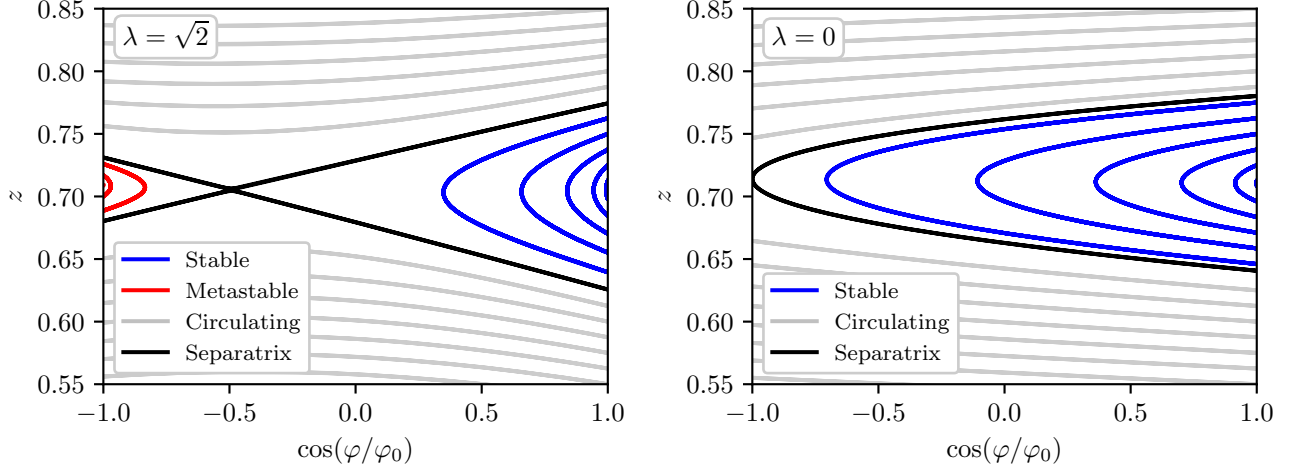


Figure 4. Phase portraits of the Bose-Bose mixture system with and without Rabi modulation, with parameters given in Table I. Each curve is obtained by numerically integrating the mean-field equations of motion (13) from different initial conditions. In the left panel, we see a family of trajectories corresponding to small oscillations around the false vacuum (red). In the right panel, we see that no such trajectories exist in the absence of the Rabi modulation.

$\mathcal{O}(\epsilon)$, we obtain first-order equations of motion to linear order in ϵ for the total and relative combinations

$$\begin{aligned} f_+ &= (1+z)f_\downarrow + (1-z)f_\uparrow, & f_- &= f_\downarrow - f_\uparrow, \\ \phi_+ &= (1+z)\phi_\downarrow + (1-z)\phi_\uparrow, & \phi_- &= \phi_\downarrow - \phi_\uparrow. \end{aligned} \quad (16)$$

Taking a second time derivative of the ϕ_\pm equations of motion, and plugging in the first-order f_\pm equations of motion, we eliminate f_\pm entirely and obtain second-order equations for the phases,

$$\partial_t^2 \begin{pmatrix} \phi_+ \\ \phi_- \end{pmatrix} = \mathbf{M} \begin{pmatrix} \nabla^2 \phi_+ \\ \nabla^2 \phi_- - \frac{4\epsilon\kappa n m}{\hbar^2} \sin \phi_- (1 + \lambda^2 \cos \phi_-) \end{pmatrix}, \quad (17)$$

where the two fields are coupled by a mixing matrix,

$$\mathbf{M} = \frac{n}{m} \begin{pmatrix} 2(g - \Delta z) - \kappa(1 - z^2) & (\kappa z - \Delta)(1 - z^2) \\ \kappa z - \Delta & \kappa(1 - z^2) \end{pmatrix}. \quad (18)$$

(Note that there are $\mathcal{O}(\epsilon)$ terms missing from this expression; capturing those would require us to include $\mathcal{O}(\epsilon^2)$ contributions in the Hamiltonian.) We see immediately that for $z = \Delta/\kappa + \mathcal{O}(\epsilon)$ the off-diagonal elements of this matrix both vanish, giving the decoupled relativistic equations of motion (7). The on-diagonal elements of \mathbf{M} then define the sound speeds of the two fields.

Vacuum fluctuations

We now consider the statistics of quantum fluctuations in the cold-atom false vacuum of our asymmetric mixture system, and show that these match the corresponding relativistic fields. This generalizes the results in Ref. [26],

which first established this equivalence for symmetric mixtures.

We promote the ψ_i from classical fields to quantum operators, and study small fluctuations around the false vacuum,

$$\hat{\psi}_\downarrow = \sqrt{n(1+z)} + \delta\hat{\psi}_\downarrow, \quad \hat{\psi}_\uparrow = -(\sqrt{n(1-z)} + \delta\hat{\psi}_\uparrow). \quad (19)$$

We work in Fourier space, and use the total and relative operators,

$$\begin{aligned} \hat{\psi}_\mathbf{k}^+ &= \int_V \frac{d\mathbf{x}}{\sqrt{2V}} e^{-i\mathbf{k}\cdot\mathbf{x}} \left(\sqrt{1+z} \delta\hat{\psi}_\downarrow(\mathbf{x}) + \sqrt{1-z} \delta\hat{\psi}_\uparrow(\mathbf{x}) \right), \\ \hat{\psi}_\mathbf{k}^- &= \int_V \frac{d\mathbf{x}}{\sqrt{2V}} e^{-i\mathbf{k}\cdot\mathbf{x}} \left(\sqrt{1-z} \delta\hat{\psi}_\downarrow(\mathbf{x}) - \sqrt{1+z} \delta\hat{\psi}_\uparrow(\mathbf{x}) \right), \end{aligned} \quad (20)$$

which are normalized so that they obey the standard bosonic commutation relations. To quadratic order in these fluctuations, the Hamiltonian (12) decouples into two independent sectors, $\hat{H}_{\text{eff}} = E_0 + \hat{H}_+ + \hat{H}_-$, if and only if the decoupling condition (6) holds. Each sector is diagonalized by a Bogoliubov transformation,

$$\hat{H}_\pm = \sum_{\mathbf{k} \neq 0} \hbar\omega_\mathbf{k}^\pm \hat{a}_\mathbf{k}^{\pm\dagger} \hat{a}_\mathbf{k}^\pm, \quad \hat{a}_\mathbf{k}^\pm = -i(u_\mathbf{k}^\pm \hat{\psi}_\mathbf{k}^\pm + v_\mathbf{k}^\pm \hat{\psi}_{-\mathbf{k}}^{\pm\dagger}), \quad (21)$$

where $u_\mathbf{k}^\pm, v_\mathbf{k}^\pm$ are real coefficients satisfying $(u_\mathbf{k}^\pm)^2 - (v_\mathbf{k}^\pm)^2 = 1$. The $\hat{a}_\mathbf{k}^{\pm\dagger}$ and $\hat{a}_\mathbf{k}^\pm$ can then be interpreted as creation and annihilation operators for the normal modes of the fields, which have energies $\hbar\omega_\mathbf{k}^\pm$.

We find that the Bogoliubov coefficients that achieve

this diagonalization are

$$\begin{aligned}(u_k^+)^2 &= (v_k^+)^2 + 1 = \frac{mc_\vartheta^2}{2\hbar\omega_k^+}(\xi_\vartheta^2 k^2 + 1) + \frac{1}{2}, \\ (\omega_k^-)^2 &= (v_k^-)^2 + 1 = \frac{mc_\varphi^2}{2\hbar\omega_k^-} \left(\xi_\varphi^2 k^2 + 1 - \frac{m_0^2}{2m^2} \right) + \frac{1}{2},\end{aligned}\quad (22)$$

and the corresponding dispersion relationships are

$$\begin{aligned}(\omega_k^+)^2 &= c_\vartheta^2 k^2 \left(1 + \frac{1}{2} \xi_\vartheta^2 k^2 \right), \\ (\omega_k^-)^2 &= \left(c_\varphi^2 k^2 + \frac{m_{\text{iv}}^2 c_\varphi^4}{\hbar^2} \right) \left(1 + \frac{1}{2} \xi_\varphi^2 k^2 - \frac{m_0^2}{4m^2} (\lambda^2 + 1) \right).\end{aligned}\quad (23)$$

On scales much larger than their respective healing lengths, $\xi_i^2 k^2 \ll 1$, these reduce to the expected relativistic expressions (massless and massive, respectively),

$$(\omega_k^+)^2 \simeq c_\vartheta^2 k^2, \quad (\omega_k^-)^2 \simeq c_\varphi^2 k^2 + \frac{m_{\text{iv}}^2 c_\varphi^4}{\hbar^2}. \quad (24)$$

In the same limit, the ϑ and φ fields themselves can be written in terms of the Bogoliubov modes as

$$\hat{\vartheta}_{\mathbf{k}} \simeq \sqrt{\frac{\hbar c_\vartheta^2}{2\omega_k^+}} (\hat{a}_{\mathbf{k}}^+ + \hat{a}_{-\mathbf{k}}^{+\dagger}), \quad \hat{\varphi}_{\mathbf{k}} \simeq \sqrt{\frac{\hbar c_\varphi^2}{2\omega_k^-}} (\hat{a}_{\mathbf{k}}^- + \hat{a}_{-\mathbf{k}}^{-\dagger}), \quad (25)$$

which match the corresponding expressions for (canonically-normalized) Klein-Gordon fields. This guarantees that the statistics of the vacuum fluctuations will match those of their relativistic counterparts in the long-wavelength regime.

One effect we have neglected here is the contribution of the zero-point energies of these Bogoliubov modes to the Hamiltonian. These Lee-Huang-Yang (LHY) terms play a vital role in studies of quantum droplet formation in Bose-Bose mixtures [45–48]. We have checked explicitly that including the resulting corrections to the equations of motion via a local density approximation does not spoil the decoupled pseudorelativistic theory described above. Instead, the LHY terms give corrections to quantities such as the sound speeds and the critical z for decoupling, which can be computed perturbatively in powers of \bar{n}^{-1} .

Euclidean bounce action

Much of the scientific insight that will be derived from analogue vacuum decay experiments will come from comparing against instanton calculations in Euclidean time $\tau = it$. These predict a decay rate per unit volume that can be written as [1, 2]

$$\frac{\Gamma}{V} \simeq A \left(\frac{B}{2\pi\hbar} \right)^{(d+1)/2} \exp(-B/\hbar), \quad (26)$$

where d is the number of spatial dimensions, A is a fluctuation determinant prefactor, and B is the Euclidean ‘bounce’ action describing the bubble nucleation event. In our effective relativistic theory, this action is given by

$$B = \int d\tau \int_V d\mathbf{x} \left(\frac{1}{2c_\varphi^2} \dot{\varphi}_b^2 + \frac{1}{2} |\nabla \varphi_b|^2 + U(\varphi_b) - U(\varphi_{\text{fv}}) \right), \quad (27)$$

where φ_b is the $O(d+1)$ -symmetric bounce solution. It is instructive to factor out all of the dimensionful quantities in this expression, to extract the overall scaling with experimental parameters. Using our definitions of m_0 , c_φ , and φ_0 , we then obtain

$$B/\hbar = \frac{\bar{n}_\varphi}{\sqrt{2}} (2\epsilon)^{(1-d)/2} (1 - z^2)^{(1+d)/2} \bar{B}, \quad (28)$$

where \bar{B} is a dimensionless bounce action that depends only on λ . As discussed in the main text, the action is proportional to the dimensionless density $\bar{n}_\varphi = n\xi_\varphi^d$, which controls the amplitude of vacuum fluctuations. We also see that, because $\epsilon \ll 1$, the action becomes parametrically larger as the number of dimensions increases, suppressing the decay rate. (Recall that this is part of our motivation for considering a 1D example setup.)

Initializing the false vacuum state

In order to realize analogue vacuum decay experimentally, we require a protocol for initializing the mixture in the appropriate metastable state, with the population imbalance chosen such that the two phase fields are decoupled. Here we sketch a simple picture of how this can be achieved by applying a strong, non-oscillating, far-detuned Rabi coupling. Assuming this coupling dominates compared to two-body interactions, the Hamiltonian can be written as

$$\hat{H} \simeq -\frac{\hbar}{2} \begin{pmatrix} |\downarrow\rangle & |\uparrow\rangle \end{pmatrix} \begin{pmatrix} \delta & \Omega \\ \Omega & -\delta \end{pmatrix} \begin{pmatrix} \langle\downarrow| \\ \langle\uparrow| \end{pmatrix}. \quad (29)$$

Here we are temporarily neglecting inhomogeneous modes, and treating the system as a superposition of the two homogeneous states $|\downarrow\rangle$, $|\uparrow\rangle$. The eigenvectors of this simplified Hamiltonian are

$$\begin{aligned}|- \rangle &\propto \Omega |\uparrow\rangle + \left(\sqrt{\delta^2 + \Omega^2} + \delta \right) |\downarrow\rangle, \\ |+ \rangle &\propto \Omega |\uparrow\rangle - \left(\sqrt{\delta^2 + \Omega^2} - \delta \right) |\downarrow\rangle,\end{aligned}\quad (30)$$

with energies $E_\pm = (\hbar/2)\sqrt{\delta^2 + \Omega^2}$. The higher-energy $|+\rangle$ state corresponds to the two species being in anti-phase, with a population imbalance that depends on the detuning,

$$z_+ = \frac{\langle +|\downarrow\rangle - \langle +|\uparrow\rangle}{\langle +|\downarrow\rangle + \langle +|\uparrow\rangle} = -\frac{\delta}{\sqrt{\delta^2 + \Omega^2}}. \quad (31)$$

Starting from a pure- $|\uparrow\rangle$ condensate ($z_+ = -1$) with a large positive detuning (or, alternatively, pure- $|\downarrow\rangle$ with a large negative detuning), one can thus achieve an antiphase state with an arbitrary population imbalance by adiabatically tuning the detuning until the desired value of z is reached. The strong Rabi coupling used to initialize the state is then replaced with the weak, modulated Rabi coupling required for the pseudorelativistic phase dynamics.

Semiclassical lattice simulations

We use a Fourier pseudospectral lattice code with an eighth-order symplectic time-stepping scheme. This code is described in detail in Ref. [26], including numerical convergence tests. Here the equations of motion and Bogoliubov spectra have been updated to capture the generalized asymmetric mixture system studied in this work. We have confirmed that this generalized version of the code performs just as well as in this previous work in terms of its numerical convergence and its conservation of the Noether charges of the cold-atom system (which are constant to within a few parts per billion throughout all of our runs).

Using this code, we perform three key tests to verify our theoretical predictions, all of which are run with our fiducial experimental parameters described in Table I:

1. We carry out runs where there are initially no fluctuations in the relative phase φ , but initialize the total phase ϑ as normal. If the two fields are decoupled, we expect φ to remain exactly homogeneous and stationary in the false-vacuum state; however, any coupling between the two fields will cause fluctuation power to leak across from ϑ to φ . If the initial population imbalance is chosen according to the procedure described in the main text, $z \sim 0.7$, we find that the variance in φ remains small throughout the run, rising to a maximum of $\sim 0.1\%$ of the mean field by the end of the simulation. This can

be interpreted as being due to a small residual coupling due to, for example, $\mathcal{O}(\epsilon^2)$ terms that we have neglected. For comparison, in runs with $z = 0$ the φ field variance grows very rapidly to equilibrate with that of the ϑ field, providing evidence of strong coupling between the two.

2. We compute dispersion relations for the fields in our simulations. This allows us to test the properties of small fluctuations around the initial state, such as the false vacuum mass and the sound speeds of the two fields. In the decoupled $z \sim 0.7$ case we find excellent agreement with our theoretical predictions, as shown in Fig. 3. In the $z = 0$ case, we find two branches of excitations when measuring the dispersion relation of either of the phase fields independently, reflecting the fact that the two are no longer decoupled. The sound speeds are also modified in this case, as expected in light of Eq. (18).
3. In order to test whether the full nonlinear dynamics of φ is consistent with a Klein-Gordon description, we compute the Noether charges of the corresponding Klein-Gordon theory (as described in Ref. [26]) and check how well these are conserved in our simulations, with any variations being interpreted as departures from perfect Klein-Gordon behavior. Some level of variation is expected due to nonrelativistic behavior on small scales, as well as renormalization corrections that have been neglected here. However, we find that the relativistic Noether charge conservation is just as good as in previous work on the symmetric case [26], and that the level of charge violation converges to zero for large \bar{n}_φ . This shows that there is a well-defined regime of Klein-Gordon behavior in the limit of small fluctuations.

Taken together, these checks provide strong numerical evidence for our prediction that a general Bose-Bose mixture exhibits decoupled pseudorelativistic dynamics if and only if the population imbalance is chosen according to Eq. (6).